The Journal of the Occanological Society of Korea
Vol. 22, No. 1, p. 9-18, March 1987.

A numerical model study on tide-induced residual currents around Chejudo Island

Yong-Hyang Park and Seong-Il Kim***

* Department of Oceanography, Cheju National University, Aradong, Cheju, Korea

** Department of Oceanography, Seoul National University, Seoul 151, Korea

제주도 주변의 조석 잔차류에 대한 수치모델 연구

박용항* · 김성일**

*제주대학교 해양학과 **서울대학교 해양학과

Abstract

A number of hydrographic studies and some recent current measurements around Chejudo Island suggest an existence of a clockwise residual flow in the west and north coasts of the island all the year round. On the eastern side of the island the Tsushima Current flows northward and northeastward.

The contribution of tide-induced residual currents to the observed residual flow around the island was examined here through numerical solution of the two-dimensional nonlinear shallow-water equations. The calculated tide-induced residual currents show a clockwise circulation around the island. Significant residuals of 2-4 cm s^{-1} are confined over sloping bottom topography around the island and the far-field residuals are negligibly small.

The inclusion of a permanent current into the model was also attempted in order to see the effects of the Tsushima Current system on the residual circulation around the island. It was found that combined effects of tide-induced residuals and the permanent current field associated with the Tsushima Current explain qualitatively not only the observed clockwise residuals in the west and north coasts but also the northward flow on the eastern side of the island.

요약 : 제주도 주변 해역에 대한 많은 해수 특성 연구와 최근의 해류 관측 결과들은 제주도 서쪽 및 북쪽 해안에 연중 존재하는 시계 방향의 잔류가 있음을 시사해 준다. 제주도 동편 해역에서는 쓰시마 해류가 북쪽과 북동쪽으로 흐른다.

이 논문에서는 2 차원 비선형 천해방정식의 수치해로 부터 구한 제주도 주변의 조석 잔차류가 관측된 잔류를 어떻게 설명할 수 있는 가를 고찰하였다. 계산된 조석 잔차류는 섬 주위에서 우선회 순환을 나타내며 섬 주위의 해저 경사 위에서만 2 ~ 4 cm·s^{-1} 의 크기로 현저히 나타나고 섬에서 멀리 떨어진 외해에서는 무시할 정도로 작다. 또한 제주도 주변의 잔류 순환에 대한 쓰시마 해류의 영향을 보기 위해 모델에 항류를 도입하여 수치 실험을 시도하였다. 이러한 수치 실험 결과, 조석 잔차류와 쓰시마 해류에 기인된 항류의 복합된 효과가 제주도 서쪽 및 북쪽 해안에서 관측된 우선회 잔류와 섬의 동쪽 해역의 북향류를 잘 설명할 수 있음이 밝혀졌다.

INTRODUCTION

There are increasing evidences for the existence of mean clockwise currents in the west and north coasts of Chejudo Island all the year round. Based on drift bottle experiments in the southern sea of Korea during the period between 1970-1972, Lee(1974) first reported that the northward flow in the west coast of the island and the eastward flow in the Cheju Strait exist throughout the year (Fig. 1). Recent hydrographic studies in the area (Kim, 1970; Kim and Lee, 1982; Park, 1986) have revealed warm and saline waters of Kuroshio origin

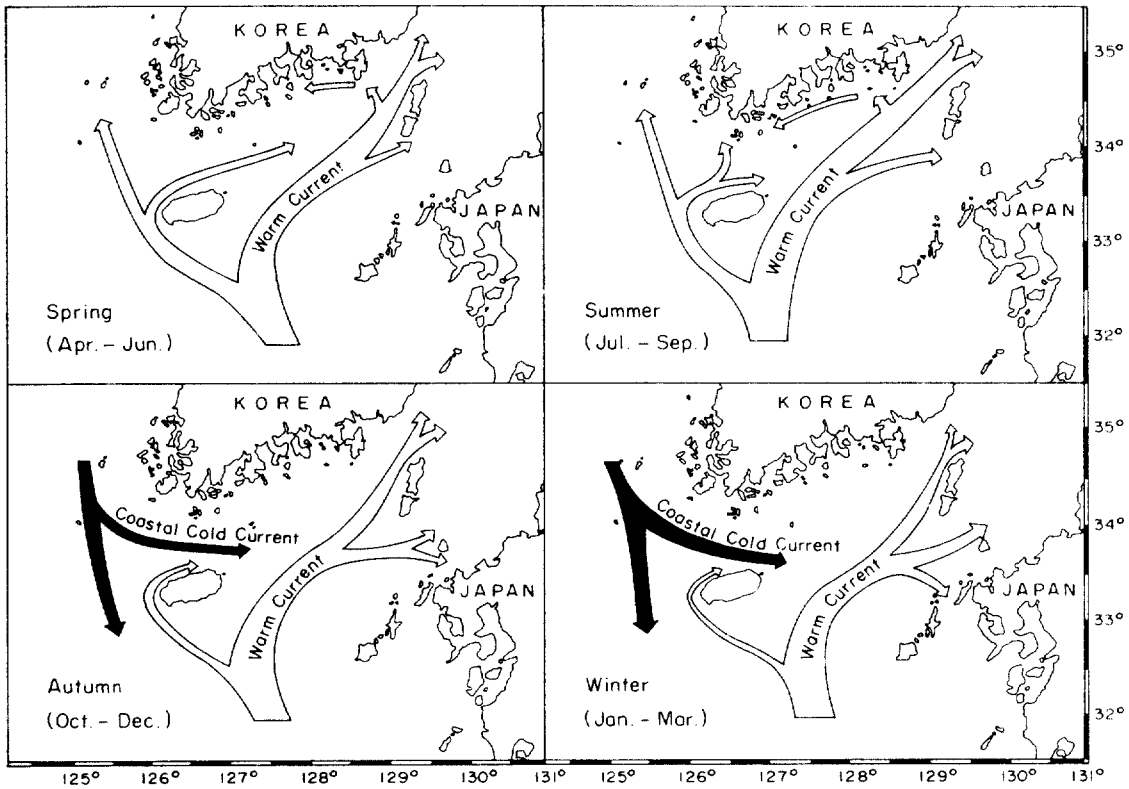

Fig. 1. Schematic maps of the seasonal surface flow in the southern sea of Korea around Chejudo Island. After Lee (1974).

distributed from the southwest to northwest coasts of the island. These hydrographic studies together with other available hydrographic data suggest strongly a consistent year round clockwise flow around the west and north coasts of the island.

The direct current measurements although they are quite limited in coverage both in time and in space show also undoubtful evidences for residual clockwise currents in this coastal area. Drogue studies during April 1983 by Chang (1984) showed northerly flow of 3-5 cm s^{-1} in the west coast of the island and easterly flow of 14-19 cm^{-1} in the northwest of the island. The fixed current meter measurements have been made mainly in the Cheju Strait, and reveal mean Eulerian currents flowing toward the northeast and east approximately parallel to the north coast of the island with speeds in the range of 5-15 cm s^{-1} during spring and summer (Kim, 1979; Chang, 1984).

On the other hand, the flow on the eastern side of the island seems to be affected mainly by the Tsushima Current which flows northward and northeastward into the Korean Strait.

It is well known that residual currents can be generated by wind stress on the sea surface, lateral density gradients due to non-uniform salinity or temperature distributions, or nonlinear interactions of the tidal streams with the local bottom or coastal topography. Wind driven residual currents which are normally intermittent and directionally inconsistent due to seasonally varying wind stresses and wind directions, could not explain adequately the observed year-round mean currents. While, tidally driven residual flows are persistent features, linked to the local bottom or coastal topography, so that they can contribute significantly

to the over-all long-term distribution and transports of water properties.

The generation of residual flows by tidal currents flowing over variable bottom topography has been the subject of a number of theoretical or numerical investigations (Huthnance, 1973; Tee, 1976; Zimmerman, 1978; Pingree and Maddock, 1979a,b; Loder, 1980). Recently Robinson (1983) reviewed the basic equations controlling the generation of residual flows through the rectification of oscillatory tidal currents by non-linear dynamics.

The major emphasis of this paper is an examination of the contribution of tidally driven residual currents to the observed residual circulation around Chejudo Island. Tide-induced residual currents around an island of simple geometry were investigated here through solution of two-dimensional non-linear tidal model. Numerical experiments were carried out for a tidally oscillating plane wave propagating across an island which has shape similar to Chejudo Island. The inclusion of a permanent current into the model was also attempted in order to take the Tsushima Current into account and to simulate more realistically the residual circulation around the island.

NUMERICAL MODEL

a. Hydrodynamic equations

The vertically-integrated hydrodynamic equations which form the basis of the model are (Heaps, 1978; Robinson, 1983):

$$\frac{\partial U}{\partial t}+\frac{\partial}{\partial x}\left(\frac{U^2}{H}\right)+\frac{\partial}{\partial y}\left(\frac{UV}{H}\right)-fV=-gH\frac{\partial \eta}{\partial x}-\frac{KU\sqrt{U^2+V^2}}{H^2}+A\nabla^2U \quad (1)$$

$$\frac{\partial V}{\partial t}+\frac{\partial}{\partial x}\left(\frac{UV}{H}\right)+\frac{\partial}{\partial y}\left(\frac{V^2}{H}\right)+fU=-gH\frac{\partial \eta}{\partial y}-\frac{kV\sqrt{U^2+V^2}}{H^2}+A\nabla^2V \quad (2)$$

$$\frac{\partial \eta}{\partial t}+\frac{\partial U}{\partial x}+\frac{\partial V}{\partial y}=0 \quad (3)$$

where the notation denotes:

- t : time,
- x,y : Cartesian coordinates in the horizontal plane of the undisturbed sea surface,
- U,V: components of transport in x, y directions
- H : Total depth of water = h + η
- h : undisturbed depth of water
- η : elevation of the sea surface
- f : Coriolis parameter
- k : coefficient of bottom friction
- g : acceleration of the Earth's gravity
- A : horizontal eddy viscosity
- ∇^2 : horizontal Laplacian operator.

b. Model formulation

In order to examine the effect of an island for the generation of residual currents in a tidally oscillating system, an idealized Chejudo Island surrounded by a uniformly sloping bottom topography is considered. The domain within which numerical computation is carried out is limited by four rectilinear open boundaries of the same length of 500 km.

The tide is introduced along the open sea boundaries by specifying elevation as a function of position and time. The problem is then to solve equations (1) — (3) to find the tidal variations of η, U, V over the sea given the changing distribution of elevation along the open boundaries. The (Eulerian) residual transport and hence the depth-mean residual current can then be obtained by taking a mean of U and V over a tidal cycle considered. Later in this paper, the input of the permanent current such as the Tsushima Current is also accomplished by prescribing adequate slopes to the open boundaries before tides are introduced.

A simple explicit finite difference method used here is a modified version from that of Ahn and Lee (1976). The grid system (staggered grid) of the model is shown in Fig. 2. It consists of three different sets of grid points: η-points denoted by a circle, U-points by a × sign and

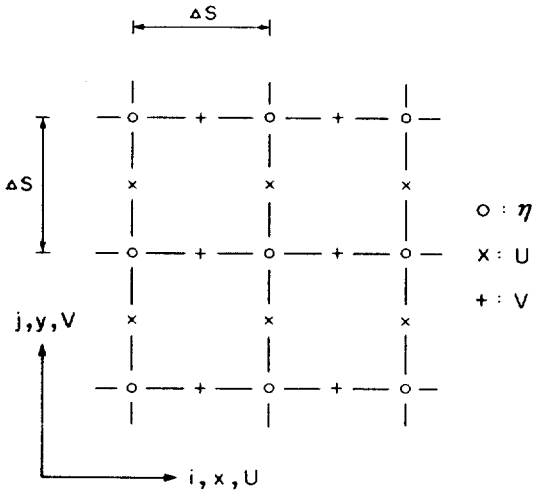

Fig. 2. Finite difference grid used in the model.

V-points by a + sign. Each of these three points has the same coordinate designation (i, j). The grid intervals Δx and Δy are chosen to be constant: $\Delta x = \Delta y = \Delta s$. The finite difference approximations for equations (1) through (3) are, using the forward method for time derivatives and the centered method for space derivatives:

$$\{\eta_{i,j}(t+\Delta t) - \eta_{i,j}(t)\}/\Delta t = -\{U_{i+1,j}(t) - U_{i,j}(t) + V_{i,j+1}(t) - V_{i,j}(t)\}/\Delta s$$

$$\{U_{i,j}(t+\Delta t) - U_{i,j}(t)\}/\Delta t = f\hat{V}_{i,j}(i) - gH^{-x}_{i,j}\{\eta_{i,j}(t+\Delta t) - \eta_{i-1,j}(t+\Delta t)\}/\Delta s - kU_{i,j}(t)\{U^2_{i,j}(t) + \hat{V}^2_{i,j}(t)\}^{1/2}/(H^{-x}_{i,j})^2 - [2\{U^{-x}_{i-1,j}(t)\}^2/(H^{-x}_{i,j} + H^{-x}_{i-1,j}) - 2\{U^{-x}_{i,j}(t)\}^2/(H^{-x}_{i-1,j} + H^{-x}_{i,j}) + U^{-y}_{i,j+1}(t)\,V^{-x}_{i,j+1}(t)/\hat{H}_{i,j} - U^{-y}_{i,j}(t)\,V^{-x}_{i,j}(t)/\hat{H}_{i,j-1}]/\Delta s + A\{U_{i+1,j}(t) + U_{i-1,j}(t) + U_{i,j+1}(t) + U_{i,j-1}(t) - 4U_{i,j}(t)\}/(\Delta s)^2$$

$$\{V_{i,j}(t+\Delta t) - V_{i,j}(t)\}/\Delta t = -f\hat{U}_{i-1,j-1}(t) - gH^{-y}_{i,j}\{\eta_{i,j}(t+\Delta t) - \eta_{i,j-1}(t+\Delta t)\}/\Delta s - kV_{i,j}(t)\{\hat{U}^2_{i-1,j-1}(t) + V^2_{i,j}(t)\}^{1/2}/(H^{-y}_{i,j})^2 - [2\{V^{-y}_{i,j-1}(t)\}^2/(H^{-y}_{i,j-1} + H^{-y}_{i,j}) - 2\{V^{-y}_{i,j}(t)\}^2/(H^{-y}_{i,j-1} + H^{-y}_{i,j}) + U^{-y}_{i-1,j}(t)\,V^{-x}_{i-1,j}(t)/\hat{H}_{i-1,j-1} - U^{-y}_{i,j}(t)\,V^{-x}_{i,j}(t)/\hat{H}_{i,j-1}]/\Delta s + A\{V_{i+1,j}(t) + V_{i-1,j}(t) + V_{i,j+1}(t) + V_{i,j-1}(t) - 4V_{i,j}(t)\}/(\Delta s)^2$$

where Δt is the time step, $H_{i,j} = h_{i,j} + \eta_{i,j}$ $(t+\Delta t)$, and for a function $F_{i,j}$ representing U, V, H the following notations mean:

$$\hat{F}_{i,j} = \frac{1}{4}(F_{i,j} + F_{i-1,j} + F_{i,j+1} + F_{i-1,j+1})$$

$$F^{-x}_{i,j} = \frac{1}{2}(F_{i,j} + F_{i-1,j})$$

$$F^{-y}_{i,j} = \frac{1}{2}(F_{i,j} + F_{i,j-1}).$$

c. *Initial and boundary conditions*

An oscillating tide is assumed to be generated from an initial state of rest $\eta = U = V = O$ at $t = O$ allowing a sufficient time for the tidal regime to become established. The non-slip condition is applied to the coastal boundary, i.e. at coast $U = V = O$. The tidal heights along the open boundaries are specified assuming a progressive plane wave of Sverdrup wave type: $\eta = \eta_0 \cos(\sigma t - \psi)$ where η_0 is the amplitude, σ the tidal frequency (e.g., M_2 frequency) and ψ is the phase in the direction of progress.

In the model experiments, the plane wave is directed from the under-right corner (SE) to the upper-left corner (NW) of the model sea, which is roughly coincident with the direction of progress of M_2 tide around Chejudo Island. The spatial distribution of the tidal heights at each time step along the open boundaries requires the knowledge of the phase speed of the tidal wave. The phase speed of Sverdrup wave on a rotating ocean of infinite dimensions is (see Defant, 1961):

$$C = \sqrt{gh}\sqrt{\frac{1}{1-S^2}}$$

where S is the ratio between the inertial and tidal frequency, $S = \frac{f}{\sigma}$. Tidal waves are only possible in this case if $S < 1$ or $\sigma > f$, and their phase speed is greater than that of Kelvin waves. In our case $S \cong 0.59$ for the M_2 wave at a mean latitude 33.5°N, which gives the phase speed $C \cong 1.23\sqrt{gh}$.

The computation of advective terms at grid points just inside the open boundaries requires

the knowledge of the transport across the boundaries. The component of transport across the open boundaries is calculated by using the continuity equation, following principally the method proposed by Oh and Choi (1986).

d. Parameter values used

The finite difference grid used in the model consists with 50×50 rectangular array elements. The grid interval is $\Delta s = 10$ km. An island (80 km in length and 40 km in width) with a regularly sloping bottom topography is placed at the centre of an ocean of constant depth, 100 m. A test was carried out imposing two different beach gradients (∇h), 1/500 and 1/300 around the island. It was found that the general circulation pattern of the residual current does not show any significant differences with these two different beach gradients, but a better space resolution appearing in the case of $\nabla h = 1/500$. In most of the following calculations $\nabla h = 1/500$ is used.

The maximum permissible time interval according to the Courant-Friedrichs-Lewy criterion ($\Delta t \leq \frac{\Delta s}{\sqrt{2gh_{max}}}$) for computational stability is 226 sec. The actual Δt used is 100 sec.

The amplitude of the M_2 plane wave, η_0 was set to be 1 m. The relative phases of the wave along the open boundaries at each instant were determined considering the phase speed of Sverdrup wave discussed previously, $C = 1.23\sqrt{gh}$, where the depth h here is equal to 100 m. Values of other parameters were taken as follows:

$f = 8.17 \times 10^{-5}\ s^{-1}$, $k = 0.0025$
$A = 100\ m^2\ s^{-1}$, $g = 9.8\ m\ s^{-2}$.

RESULTS

After computing through 12 periods of the M_2 tide the stable tidal regime had become established such that there were no significant differences in the elevation and the velocity from the 11th to 12th cycle. Data from 12th period were then taken as the required solution.

a. Amplitude and phase of the M_2 wave

Fig. 3 shows the calculated M_2 amplitude and phase distribution around the island. It is interesting to remark that the phase lines of the plane wave which propagates originally from SE to NW are modified drastically around the island. Around the northeastern and southwestern corners of the island the phase lines are concentrated and the extreme depression and elevation in amplitude appear around these concentrated phase lines.

This pattern of the amplitude and phase distritribution is consistent with the numerical model results by Kim and Lee (1986) who investigated recently the scattered M_2 wave around Chejudo Island. According to them the differential variation of the amplitude can be well explained by the diffraction of an incident wave. Due to the Coriolis force the larger and smaller amplitudes than the incident wave's appear on the coast right and left of the wave propagation, respectively, in the northern hemisphere. They showed that the normalized

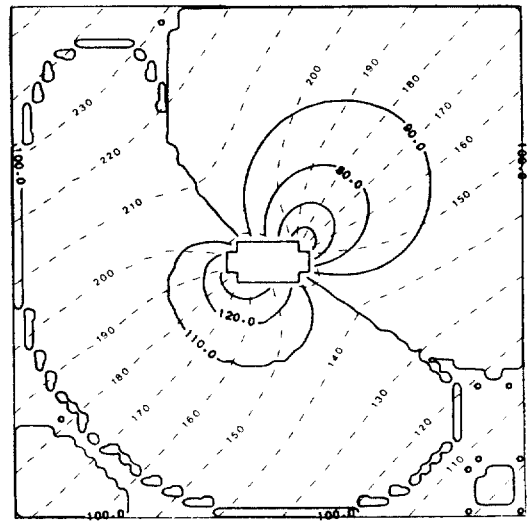

Fig. 3. Calculated M_2 amplitude in cm (solid lines) and phase in degree (dotted lines). The amplitude of the incident plane wave along the open boundaries was set to be 100 cm. The phase is relative to an arbitrary origin.

amplitude relative to the incident wave lies in the range of 0.8 and 1.2 approximately. In our case the highest amplitude on the southwestern corner is ∿130 cm and the lowest amplitude on the northeastern corner is ∿60 cm so that the normalized amplitude lies in the range of 0.6 and 1.3. A much higher deviation of the scattered wave from the incident wave in the present model compared to that of Kim and Lee (1986) seems to be related to different topographic specifications in the two models. In Kim and Lee's plane wave model an elliptical island without beach gradient was considered while in our case we introduced a beach gradient of 1/500 around the island. A test with a steeper beach gradient of 1/300 (not shown here) revealed somewhat reduced normalized amplitude approaching to theoretical values proposed by Kim and Lee (1986).

b. Tide-induced residual currents

The residual current $\vec{V}_R$ was calculated by integrating the current $\vec{V}$ over M_2 period T,

$$\vec{V}_R = \frac{1}{T}\int_0^t \vec{V}dt$$

Fig. 4 shows the calculated tide-induced residual currents around the island with the beach

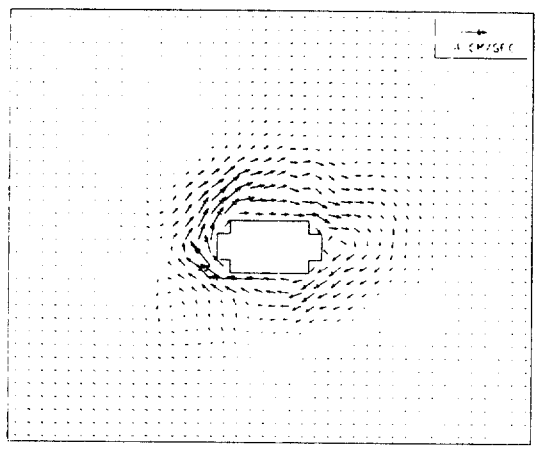

Fig. 4. Tide-induced residual currents calculated in the model with $\nabla h = 1/500$ and considering all the terms in the equation of motion. The boundary of the sloping beach is situated in five grid points from the island.

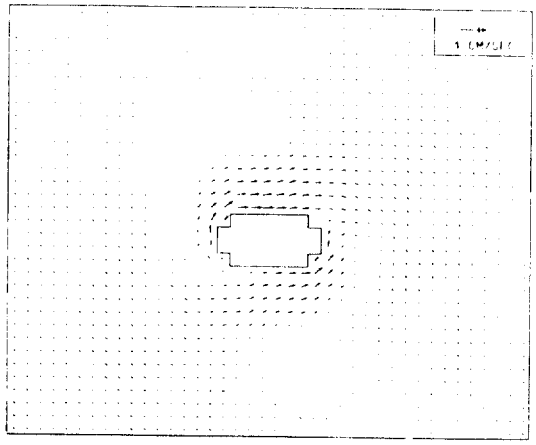

Fig. 5. Tide-induced residual currents calculated in the model with $\nabla h = 1/500$ and neglecting the advective terms.

gradient, $\nabla h = 1/500$. The most striking features of the flow are the clockwise circulating high-velocity residuals over the sloping bottom topography around the island. A similar result was obtained with $\nabla h = 1/300$ (not shown here).

The strongest residual current are ∿4 cm s^{-1} in the west coast of the island and the far-field residuals are negligibly small. The amplitude of the tidal current in the present model is ∿40 cm s^{-1} so that the maximum residual current is about 10% of the tidal current. There appears an asymmetry in the residual flow around the island showing relatively stronger and narrower residuals on the western side of the island than their counter parts on the eastern side.

In order to examine the effects of different terms in the equation of motion on the calculated clockwise residual currents shown in Fig. 4, the computation was performed first neglecting the advective terms (Fig. 5) and second neglecting the Coriolis terms (Fig. 6). It can be easily seen that neglecting the advective terms changes drastically the strength of the residual current. The values of $\vec{V}_R$ around the island are reduced from the order of 3 cm s^{-1} to less than 1 cm s^{-1}. The far-field residual currents are still negligibly small.

In the case of neglecting the Coriolis terms the residual current field shows completely dif-

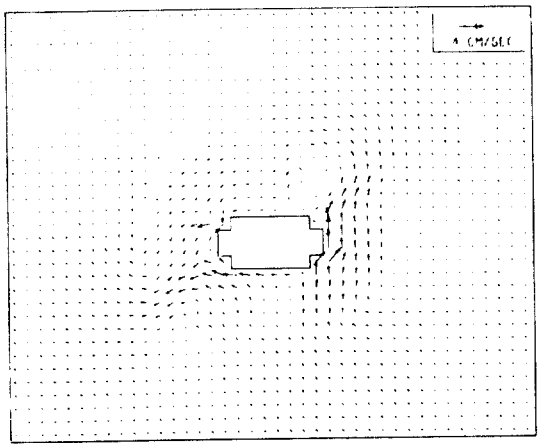

Fig. 6. Tide-induced residual currents calculated in the model with $\nabla h = 1/500$ and neglecting the Coriolis terms.

ferent pattern from that shown in Fig. 4. Instead of circulating clockwise around the island the residual currents are directed to the north in the east coast and to the west in the north and south coasts. In the west coast the residual currents are much weaker than those in the east coast and they are directed to the southwest.

These results indicate obviously that the residual current is generated mainly by the inertial effect and that the clockwise residual flow in Fig. 4 is due to the Coriolis force.

DISCUSSION

It has been shown from the results of numerical experiments that noticeable tide-induced residual currents can be produced by inertial force over the sloping bottom topography around the island. This is not suprising because significant residual flows can be generated by vorticity associated primarily with the rate of stretching of water columns moving over depth variations and secondly with the bottom frictional torque. In the absence of any topographic features, i.e. $\nabla h = O$, vorticity will still be generated weakly by the tidal motion because of $\Delta\eta$ in the vorticity equation but its magnitude will be 2-3 orders of magnitude less than for the topographically induced cases (Robinson, 1983).

When the effects of Earth's rotation are considered the tide-induced residual currents show a clockwise circulation around the island (Fig. 4) and this can be compared with the observed flow pattern around Chejudo Island. The directions of calculated residual currents seem to be consistent with the observed year-round clockwise flow around the west and north coasts of Chejudo Island, however, they are opposite from the observed northward flow on the eastern side of the island (see Fig. 1). On the eastern side of the island the flow seems to be affected mainly by the Tsushima Current which flows northward and northeastward into the Korean Strait.

In order to take the Tsushima Current into account and to simulate a more realistic residual circulation around the island the input of the permanent current into the model has been attempted. To simulate the typical transport of 2×10^6 m^3 s^{-1} of the Tsushima Current out of

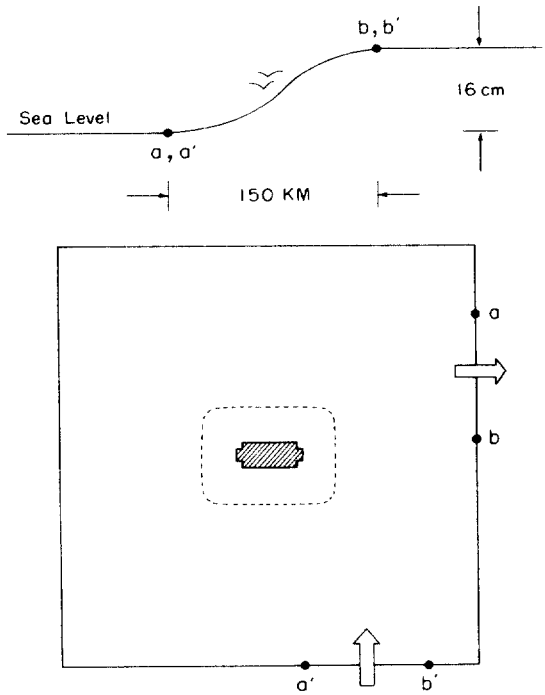

Fig. 7. Specification of an artificial sea-level difference along the eastern (a-b) and southern (a'-b') boundaries. This specification is designed in order to include a permanent current (Tsushima Current) into the model.

the Korean Strait, a sea-level difference of 16 cm in the distance of 150 km following a half-sine curve was specified along the northern part of the eastern boundary before tides are introduced (Fig. 7). A similar sea-level variation was also taken into consideration along the eastern part of the southern boundary, which could translate into the northward flow of the same transport through the southern entrance. The other parts of the open boundaries were set to be level and computations were then made until the steady-state was reached in the model sea.

Fig. 8 shows the calculated residual current field from the model driven by tides and time-invariant sea-level slopes. The figure may be interpreted to simulate a strong inflow of the Tsushima Current into the model sea from the southeast and a strong outflow of the current to the northeast. It is interesting to remark that the currents around the southern entry (A) diverge radially while those around the eastern exit (B) converge. Strongest currents are directed northward from the southeast to the east of the island and they turn gradually to the northeast and east to exit through B. In the west and northwest coasts of the island a clockwise

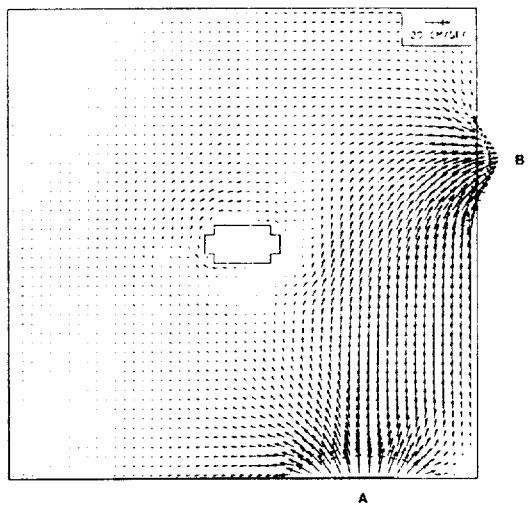

Fig. 8. Pattern of the residual current from the model driven by tides and time-invariant sea-level slope specified as in Fig. 7.

turning of currents of noticeable magnitudes (3-5 cm s^{-1}) can be seen while the clockwise residual currents in the east coast seen in Fig. 4 have now been disappeared. This may be due to the combined contributions of tidally driven residuals and steady-state currents associated with the Tsushima Current system. On the western side of the island northward steady currents derived from the Tsushima Current (branching from A) will be combined with the clockwise tidal residuals producing a little intensified northward and northeastward flow around the west and northwest coasts of the island. While on the eastern side of the island the Tsushima Current flows northward in the opposite direction of the clockwise tidal residuals so that current directions there are determined by the stronger Tsushima Current.

This calculated residual current field (Fig. 8) seems to accord qualitatively with the hitherto believed residual currents around Chejudo Island (Fig. 1). Based on our numerical experiments it can be said that the observed year-round clockwise mean currents around the west coast of the island may be due primarily to tidally driven residuals and secondly to steady-currents associated with the Tsushima Current system. The order of magnitude of calculated residuals in the west coast of the island ($\sim$4 cm s^{-1}) appears to be in agreement with that from the drogue experiments by Chang (1984) who showed northerly flow of 3-5 cm s^{-1} in the area.

However, we could not succeed in the simulation of the stronger residuals in the north coast of the island where the observed residuals are much stronger (5-15 cm s^{-1} by Kim, 1979 and Chang, 1984) than in the west coast. The calculated residual currents here are less than 3 cm s^{-1} (see Fig. 8), so that the observed strong residuals in the Cheju Channel can not be explained with the present simple model. The stronger eastward residuals in the Cheju Channel are presumably related to some eastward transport of waters through the western entrance of the channel. Lack of knowledge about this transport and the eventual complication in

the formulation of the model especially in the determination of boundary conditions when the Cheju Channel is considered in the model, limit us to proceed to challenge the problem.

Another disadvantage of the present model seems to be in the fact that the calculation grid size (10 km) is relatively coarse compared with the variation of local bottom topography around the island (10-30 km). In our case the choice of finer grid size is economically limited.

Besides the imperfect simulation of residuals in the north coast of the island, however, our model seems to demonstrate the basic features of residual currents around Chejudo Island.

CONCLUSIONS

Tide-induced residual currents from the two-dimensional nonlinear model show a clockwise circulation around the island. The maximum speed of these residual currents is $\sim$4 cm s^{-1} in the west coast of the island which is about 10% of the amplitude of tidal currents. Significant tide-induced residual currents of 2-4 cm s^{-1} are confined over a sloping bottom topography around the island and the far-field residuals are negligibly small.

The clockwise circulation associated with tide-induced residual currents may explain qualitatively the observed clockwise flow in the west and north coasts of Chejudo Island but it does not accord with the northward flow along the east coast of the island. The inclusion of the Tsushima Current into the model produced a little intensification of clockwise residual currents in the west and northwest coasts of the island and a general northward flow on the eastern side of the island. These results compare better with the observations.

It is inferred from our numerical experiments that the observed residual currents around Chejudo Island are closely related to the combined effects of the tide-induced residual currents and the Tsushima Current system. The clockwise flow in the west and northwest coasts of the island seems to be mainly due to the contribution of tide-induced residual currents while the northward flow on the eastern side of the island is thought to be dominated by the Tsushima Current.

From the present simple model the observed strong residual currents in the Cheju Channel could not be explained. A more sophiscated model which take the Cheju Channel and the actual geometry of the area into account will be desirable in the future study.

ACKNOWLEDGEMENTS

The work is carried out during the visit of one of the authors (Park) in the Department of Oceanography, Seoul National University during 1986. Financial support is given from a research fund of the Ministry of Education.

REFERENCES

Ahn, H.S. and S.W., Lee. 1976. A numerical experiment on tidal currents in Asan Bay. J. Oceanol. Soc. Korea, **18:** 18-24.

Defant, A. 1961. Physical oceanography. Vol. II. Pergamon Press, 598 pp.

Heaps, N.S. 1978. Linearized vertical-integrated equations for residual circulation in coastal seas. Deutsche Hydrographishe Zeitschrift, Jahrgang 31, Heft **5:** 147-169.

Huthnance, J.M. 1973. Tidal current assymetries over the Norfork sanbanks. Estuarine and Coastal Marine Science, **1:** 89-99.

Jang, K.I. 1984. The structures of currents and its flow dynamics of the Jeju Strait. M.S. Thesis, Seoul National University, 62 pp.

Kim, B.K. 1979. A study on the currents in the Cheju Strait. Bull. Fish. Res. Dev. Agency, Korea, **21:** 7-21.

Kim, K. 1980. Ocean currents in southwestern sea of Korea. Unpublished technical report, Seoul National University.

Kim, K. and S.H., Lee. 1982. Vertically homogeneous water along the west coast of Jeju Island. J. Oceanol. Soc. Korea, **17:** 59-68.

Kim, K. and S.H., Lee. 1986. Variation of the M_2 tide amplitude around the Jeju-Do. J. Oceanol. Soc. Korea, **21:** 171-183.

Lee, C.K. 1974. The drift bottle experiment in the southern sea of Korea. Bull. Fish. Res. Dev. Agency, Korea, **3:** 7-26.

Loder, J.W. 1980. Topographic rectification of tidal currents on the sides of George Bank. J. Phys. Oceanogr., **10:** 1399-1416.

Oh, I.S. and H.W., Choi. 1986. A study on open boundary condition for tidal current model. J. Korean Earth Sci. Soc., **7:** 35-45.

Park, Y.H. 1986. Water characteristics and movements of the Yellow Sea Warm Current in summer. Submitted to the Deep-Sea Research.

Pingree, R.D. and L. Maddock. 1979a. The tidal physics of headland flows and offshore tidal bank formation. Mar. Geol., **32:** 269-289.

Pingree, R.D. and L. Maddock. 1979b. Tidal flow around an island with a regularly sloping bottom topography. J. Mar. Biol. Assoc. U.K., **59:** 699-710.

Robinson, I.S. 1983. Tidally induced residual flows. in Physical oceanography of coastal and shelf seas edited by B. Johns, Elsevier Science Pub.: 321-356.

Tee, K.T. 1976. Tide-induced residual current, a 2-D nonlinear numerical tidal model. J. Mar. Res., **34:** 603-628.

Zimmerman, J.T.F. 1978. Topographic generation of residual circulation by oscillatory (tidal) currents. Geophys. Astrophys. Fluid Dynamics, **11:** 35-47.

Received January 5, 1987
Accepted February 5, 1987